Optical characterization of two-dimensional array of 2048 tilting micromirrors for astronomical spectroscopy

Michael D. Canonica, Frederic Zamkotsian, Patrick Lanzoni, Wilfried Noell, Nico de Rooij

Optical characterization of two-dimensional array of 2048 tilting micromirrors for astronomical spectroscopy

Michael D. Canonica,[1,2] Frédéric Zamkotsian,[3*] Patrick Lanzoni,[3] Wilfried Noell,[1] and Nico De Rooij[1]

[1] *Institute of Microtechnology, Ecole Polytechnique Fédérale de Lausanne, Jaquet-Droz 1, CH-2002 Neuchâtel, Switzerland*

[2] *Currently with the Department of Aeronautics and Astronautics, Massachusetts Institute of Technology, 77 Massachusetts Avenue, Cambridge, MA 02139, USA*

[3] *Laboratoire d'Astrophysique de Marseille, 38 rue Frédéric Joliot Curie, F-13388 Marseille Cedex 13, France*

[*] *frederic.zamkotsian@oamp.fr*

Abstract: A micromirror array composed of 2048 silicon micromirrors measuring 200 x 100 μm^2 and tilting by 25° was developed as a reconfigurable slit mask for multi-object spectroscopy (MOS) in astronomy. The fill factor, contrast, and mirror deformation at both room and cryogenic temperatures were investigated. Contrast was measured using an optical setup that mimics a MOS instrument, and mirror deformation was characterized using a Twyman-Green interferometer. The results indicate that the array exhibited a fill factor of 82%, a contrast ratio of 1000:1, and surface mirror deformations of 8 nm and 27 nm for mirrors tilted at 298 K and 162 K, respectively.

OCIS codes: (230.3990) Micro-optical devices; (230.4685) Optical microelectromechanical device; (350.1260) Astronomical optics.

References and links

1. J. B. Hearnshaw, "Astronomical spectrographs and their history," (Cambridge University Press, 2009), http://www.cambridge.org/9780521882576.
2. W. Saunders, G. Smith, J. Gilbert, R. Muller, M. Goodwin, N. Staszak, J. Brzeski, S. Miziarski, and M. Colless "MOHAWK: a 4000-fiber positioner for DESpec," Proc. SPIE **8486**, 84464W (2012), http://dx.doi.org/10.1117/12.925724.
3. P. Spanoudakis, L. Giriens, S. Henein, L. Lisowski, A. O'Hare, E. Onillon, P. Schwab, and P. Theurillat "Configurable slit-mask unit of the Multi-Object Spectrometer for Infra-Red Exploration for the Keck telescope: Integration and tests," Proc. SPIE **7018**, 70180I (2008), http://dx.doi.org/10.1117/12.789017.
4. M. J. Li, A. D. Brown, A. S. Kutyrev, H. S. Moseley, and V. Mikula "JWST microshutter array system and beyond," Proc. SPIE **7594**, 75940N (2010), http://dx.doi.org/10.1117/12.843728.
5. J. B. Stewart, T. G. Bifano, S. Cornelissen, P. Bierden, B. M. Levine, and T. Cook, "Design and development of a 331-segment tip-tilt-piston mirror array for space-based adaptive optics," Sens. Act. A, **135**, 230-238, (2007), http://dx.doi.org/10.1016/j.sna.2007.04.051
6. J. H. Park, G. K. Garipov, J. A. Jeon, B. A. Khrenov, J. E. Kim, M. Kim, Y. K. Kim, C.-H. Lee, J. Lee, G. W. Na, S. Nam, I. H. Park, and Y.-S. Park "Obscura telescope with a MEMS micromirror array for space observation of transient luminous phenomena or fast-moving objects, Optics Express, **16**, 25, 20249-57, (2008), http://dx.doi.org/10.1364/OE.16.020249

#193788 - $15.00 USD Received 17 Jul 2013; revised 29 Aug 2013; accepted 29 Aug 2013; published 16 Sep 2013

7. S. M. Weber, L. Bonacina, W. Noell, D. Kiselev, J. Extermann, F. Jutzi, S. Lani, O. Nenadl, J.-P. Wolf, and N. F. de Rooij "Design, simulation, fabrication, packaging, and characterization of a MEMS-based mirror array for femtosecond pulse-shaping in phase and amplitude, Rev. Sci. Instrum., **82**, 7, 075106, (2011), http://dx.doi.org/10.1063/1.3606440
8. R. D. Meyer, K. J. Kearney, Z. Ninkov, C. T. Cotton, P. Hammond, and B.D. Statt "RITMOS: A micromirror-based multi-object spectrometer," Proc. SPIE **5492**, 200 (2004), http://dx.doi.org/10.1117/12.549897.
9. J. W. MacKenty, R. G. Ohl, M. A. Greenhouse, and R. F. Green "Commissioning of the IRMOS MEMS spectrometer," Proc. SPIE **6269**, 626915 (2006), http://dx.doi.org/10.1117/12.672317.
10. F. Zamkotsian, P. Lanzoni, E. Grassi, R. Barette, C. Fabron, K. Tangen, L. Valenziano, L. Marchand, and L. Duvet "Successful evaluation for space applications of the 2048 x 1080 DMD, Proc. SPIE **7932**, 79320A (2011), http://dx.doi.org/10.1117/12.876872
11. M. D. Canonica, F. Zamkotsian, P. Lanzoni, W. Noell, and N. De Rooij "The two-dimensional array of 2048 tilting micromirrors for astronomical spectroscopy," J. Micromech. Microeng. **23**, 055009 (2013), http://dx.doi.org/10.1088/0960-1317/23/5/055009.
12. A. M. Michalicek and V. M. Bright "Flip-chip fabrication of advanced micromirror arrays," Sens. Act. A **95**, 15267 (2002), http://dx.doi.org/10.1016/S0924-4247(01)00726-9.
13. F. Zamkotsian, J. Gautier, and P. Lanzoni "Characterization of MOEMS devices for the instrumentation of next generation space telescope," Proc. SPIE **4980**, 324 (2003), http://dx.doi.org/10.1117/12.478210.
14. F. Zamkotsian, E. Grassi, S. Waldis, R. Barette, P. Lanzoni, C. Fabron, W. Noell, and N. De Rooij "Interferometric characterization of MOEMS devices in cryogenic environment for astronomical instrumentation," Proc. SPIE **6884**, 68840D (2008), http://dx.doi.org/10.1117/12.768410.

1. Introduction

To map the Universe, and further understand the formation of galaxies, astronomers use a technique called multi-object spectroscopy (MOS), which permits the simultaneous collection of spectra of many stars and galaxies. These spectrographs, which are mounted in space or ground telescopes, are equipped with slit masks placed in the focal plane of the telescope, allowing astronomical object selection. Using MOS, spoiling sources and sky background emission can be removed from the observation, potentially enabling the simultaneous study of multiple faint objects. Different types of slit masks were previously developed for object selection, including conventional slit-masks [1], fiber-based slit masks [2], sliding bar-based slit masks [3], and microshutter arrays [4].

In the last few decades, micromirror arrays (MMA) enable enhancements for a wide-variety of applications such as wavefront correction error [5], Earth Observation [6], pulse-shaping [7], etc. For MOS, MMA can improve the capabilities of the spectrometers by operating as a real-time reconfigurable slit mask. MMA enable object selection by tilting the micromirrors between two positions: when the micromirrors are at rest (OFF state), the light of non-selected objects and sky background is sent back to space; when the micromirrors are tilted (ON state), the light of objects are reflected towards the spectrometer and the spectra of these objects are obtained.

Based on this principle and the use of a commercially available digital micromirror device (DMD) from Texas Instruments, some groups successfully developed MOS instruments [8, 9]. However, previous studies demonstrated that the lowest operating temperature of the large format DMD (2048 x 1080) is -40°C [10], thereby hindering cryogenic operation, which is required to minimize instrument background noise during the collection of the mid- and far-infrared spectrum. Furthermore, with an off-the-shelf device, parameters such as micromirror dimensions or tilt angle cannot be tailored for the application.

Therefore, for several years, our team has been developing MMA dedicated as reconfigurable slit masks for MOS. For the observation of faint objects, our arrays have to achieve the following: high fill factors ($>80\%$), high contrast ratio ($>$1000:1), peak-to-valley (PTV) mirror deformation of at least $\lambda/20$ for a typical wavelength of 1 μm, and cryogenic operation.

In this letter, we present the optical properties, namely the fill factor, contrast level, and mirror deformations at both room temperature (RT) and cryogenic temperatures for a MMA composed of 2048 tilting micromirrors measuring 200 x 100 μm^2 [11].

#193788 - $15.00 USD Received 17 Jul 2013; revised 29 Aug 2013; accepted 29 Aug 2013; published 16 Sep 2013

2. Concept and fabrication

The micromirror cell is based on an electrostatic double plate actuator, and is composed of two parts: an electrode chip, and a mirror chip as illustrated in Fig. 1(a). The bulk silicon mirror is attached to the frame via flexure beams. The stopper beam and the two landing beams provide a precise tilt angle when the micromirror is tilted [12]. The electrostatic gap between the electrode and the mirror is precisely defined by pillars. When the voltage between the mirror and the electrode is larger than the pull-in voltage, the micromirror tilts toward the electrode and stays electrostatically clamped at a precise tilt angle, as described in Figs. 1(b)–1(d).

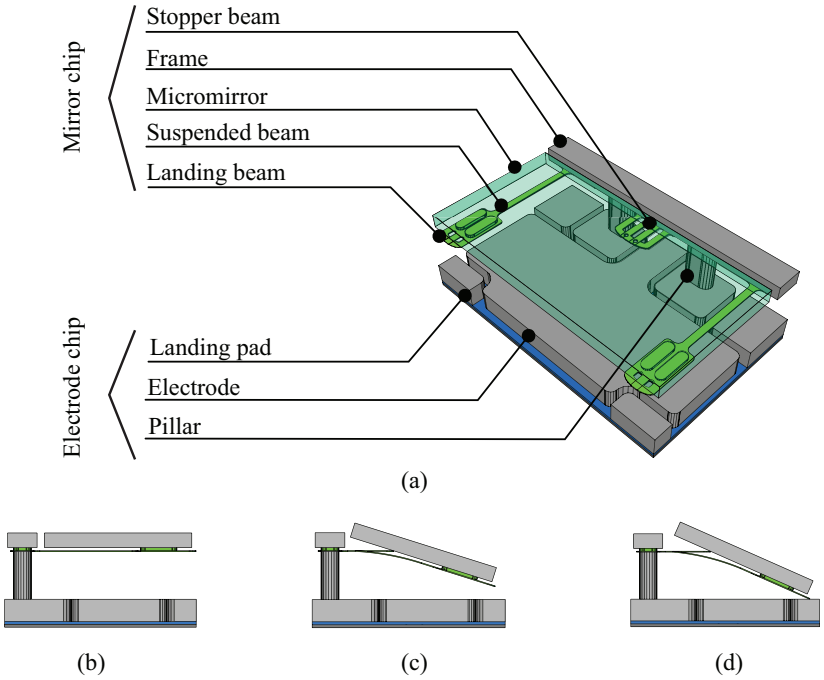

Fig. 1. (a) A micromirror cell has a system of beams achieving a precise tilt angle after actuation. (b) At rest, when no voltage was applied, the micromirror was held in a flat position. (c-d) At the pull-in voltage, the micromirror was tilted towards its electrode. During this motion, the micromirror first touched its stopper beam, and subsequently its landing pads.

The fabrication of these MMA required the use of bulk processing, surface micromachining and wafer-level bonding. To make these devices, 3 wafers, 8 lithography masks and 2 wafer-level bondings were necessary. A fabricated MMA is shown in Fig. 2. The fabrication process was optimized to ensure a high degree of uniformity throughout the wafer, and to enable the fabrication of larger arrays without major modifications to the process. A detailed description of the fabrication process can be found elsewhere [11].

The micromirrors were controlled via custom-made external electronics based on the digital-to-analog converter (DAC) AD5535 from Analog Devices, which are composed of 128 channels ranging from 0 to 148 V. A microcontroller, was used to send the voltage values to the DAC from a MATLAB user interface.

#193788 - $15.00 USD Received 17 Jul 2013; revised 29 Aug 2013; accepted 29 Aug 2013; published 16 Sep 2013

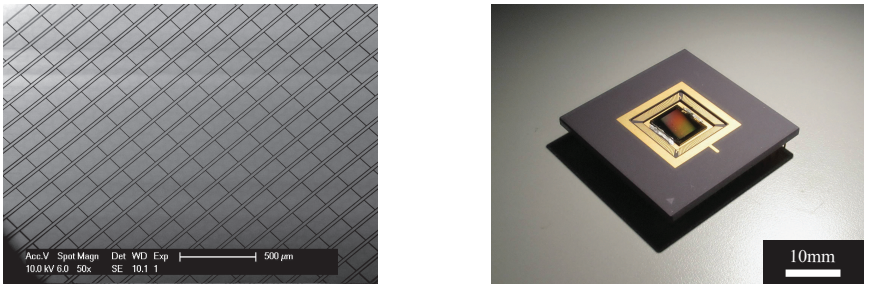

(a) (b)

Fig. 2. MMA of 2048 micromirrors (32 x 64) measuring 200 x 100 x 10 μm^3. (a) Scanning Electron Microscope (SEM) image of the surface of the mirrors at the end of the fabrication. (b) Packaged and wirebonded MMA.

3. Results

For the optical characterization, an array composed of 32 x 64 silicon micromirrors measuring 200 x 100 μm^2 and tilting by 25° was used. This array was line-addressed, meaning that all 32 micromirrors of each line had a single electrode and were simultaneously tilted when a voltage was applied.

3.1. Fill factor

The fill factor of a MMA is defined by the ratio between the surface area of the mirror and of the micromirror cell, which includes the mirror itself, the frame, and the gaps around the micromirrors, as described in Fig. 1(a). Also, for MOS, the fill factor has to be maximized to achieve full coverage of the field of view. The fill factor was defined during the design of the array, however due to fabrication process variations, its real value has to be precisely characterized. By measuring the dimensions of the gap around a micromirror using a SEM, a fill factor of 82% was obtained for the processed devices. Moreover, since there is no frame in the long slit mode direction (along the long side of the micromirror), a filling ratio of as high as 98% was obtained.

3.2. Contrast

The contrast of a micromirror was measured on a dedicated optical bench that mimicked an astronomical object, a telescope, and a spectrograph [13]. Figure 3 shows the optical bench for the contrast measurement. The astronomical object was mimicked by a polychromatic light source (S1) which was collimated by a lens (L1), while the telescope was simulated by a lens (L2) and the input pupil (P1). The spectrograph was mimicked by a lens (L3), the output pupil (P2) and another lens (L4). By varying the size of the input pupil (P1), it was possible to change the F-number of the telescope, and allow the measurement of the contrast at different F-numbers. The output pupil (P2) was used to simulate the grating location, which also influences the throughput of the system. When the size of the output pupil is limited, such as in a space telescope, the pupil filters the diffracted light generated by the micromirrors and thereby reduces the throughput and contrast of the system. Therefore, to avoid pupil oversizing or a decrease in throughput and contrast, the MMA has to minimize the diffracted light by having micromirrors with low roughness, low deformation, and small gaps between mirrors. Finally, for characterizing the diffraction effects, input and output pupils were imaged on the detector (D2) using a lens (L5).

The polychromatic light source (S1) was focused to a diameter of 200 μm on a micromirror,

#193788 - $15.00 USD Received 17 Jul 2013; revised 29 Aug 2013; accepted 29 Aug 2013; published 16 Sep 2013

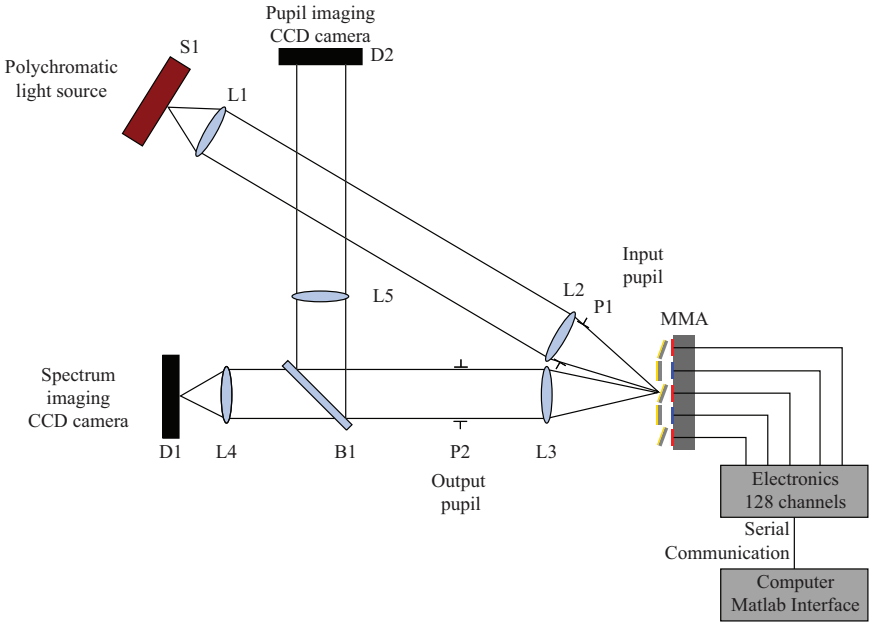

Fig. 3. Optical setup for the contrast characterization of a micromirror. The polychromatic light source (S1) and lens (L1) simulated an astronomical object; the lens (L2) and the input pupil (P1) simulated the telescope; the lens (L3), output pupil (P2) and the other lens (L4) simulated the spectrograph. The pupils were imaged on the detector (D2).

a diameter which corresponds to the typical plate scale (at the focal plane of next-generation telescopes) of a galaxy having an angular size of 0.5" in the sky, as depicted in Fig. 4(a). The input pupil (P1) was set to F/4, which is the most challenging configuration for the contrast measurement, but it provides the largest field of view. Using a charge coupled device (CCD) camera with a spatial resolution of 2.25 μm/pixel in the field of view, the intensity of the reflected light was integrated when the line of this mirror, and the two neighboring lines, were both tilted and at rest, as shown in Figs. 4(b) and 4(c). The contrast was defined as the ratio between the integrated intensity over the mirror surface at rest and tilted [13]. In the tilted state, the exposure time was 0.1 s. However, in the rest state, since the light only comes from reflection of the micromirror edges and electrode, the exposure time was increased to 10 s, in order to maximize the signal-to-noise ratio at the detector. The contrast was then obtained by calculating the ratio between these two integrated intensities, with compensation for the difference in exposure times, leading to a contrast ratio of about 1000:1 for a micromirror with a tilt angle of 25°.

Typically, a contrast of 1000:1 is sufficient to remove the background noise generated by the sky and common spoiling sources. If necessary, higher contrast can be obtained by decreasing the F-number, decreasing the gap between the mirrors, and coating the electrode with an anti-reflective coating.

3.3. Micromirror deformation

3.3.1. Optical setup

The deformation of the micromirrors at RT and cryogenic temperatures was characterized by placing the line-addressed MMA in a cryogenic chamber, which was mounted in front of a

#193788 - $15.00 USD Received 17 Jul 2013; revised 29 Aug 2013; accepted 29 Aug 2013; published 16 Sep 2013

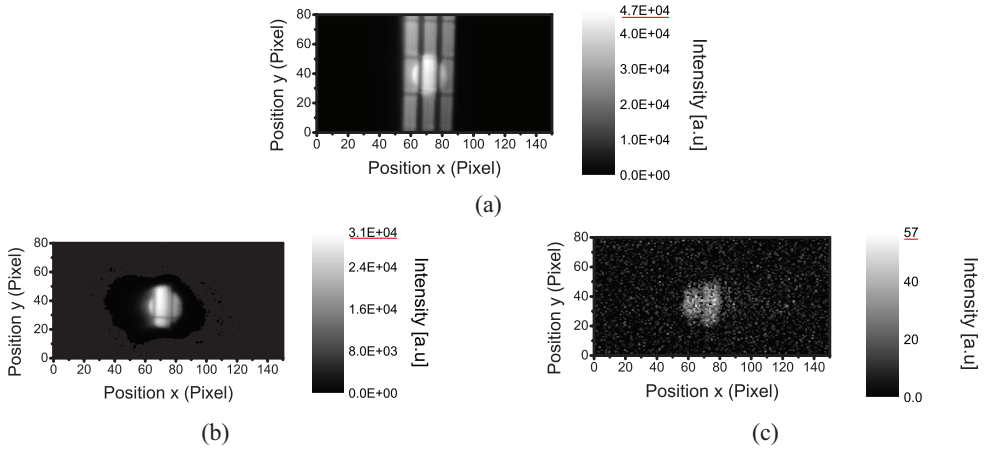

Fig. 4. The contrast was obtained by focusing a 200 μm diameter light source on 3 lines of 32 micromirrors, and subsequently measuring the integrated intensity over the micromirror surface for the rest and tilted states. (a) 3 tilted lines of micromirrors illuminated by an external source and the 200 μm diameter light source aimed at the micromirror. (b) Intensity measurement when the 3 lines of micromirrors were tilted (ON state) for an exposure time of 0.1 s. (c) Intensity measurement when the 3 lines of micromirrors were at rest (OFF state) for an exposure time of 10 s. In this case, the measured light comes from reflection of the micromirror edges and of the electrode.

Twyman-Green interferometer, as described in Fig. 5 [14]. This type of interferometer uses a low coherence light source (λ =650 nm, $\Delta\lambda$ =10 nm) for characterizing the deformation of optical components. To characterize the micromirrors in their rest state as well as their tilted state, the chamber was mounted on a rotating stage and the MMA placed in a precisely controlled orientation. By rotating the chamber to the value of the micromirror tilt angle (25°), it was possible to quantify the surface quality of the tilted micromirrors *in-situ*. However, when the MMA was tilted, only a line of micromirrors could be measured at once due to the low coherence of the light.

To balance variations of dimensions at cryogenic temperatures, the packaged MMA was clamped in a zero-insertion-force socket mounted on a dedicated printed circuit board that was fixed in the chamber via a point-plane-plane attachment system. The MMA was electrically supplied via a 100 pin feedthrough and the chamber was closed by a flange equipped with a high-quality glass window (W1). To achieve an optimal fringe contrast and nanometer resolution, a compensating plate (W2) identical to the glass in (W1) was placed in the reference arm of the interferometer.

After cooling, the system reached thermal equilibrium at 162 K and at the pressure of 10^{-6} mbar. This temperature was limited by the capability of the cryopump and the thermal insulation of the chamber.

3.3.2. Cryogenic behavior

For this experiment, out of the 17 working lines that contain 32 micromirrors each, 3 contiguous lines were selected as the exemplary system and are depicted in Fig. 6(a). The electromechanical behavior of these lines was characterized at three conditions: before (at RT), during (at 162 K), and after (at RT) the cryogenic test described earlier. Before cooling the chamber, each micromirror could be tilted by 25° using a voltage of 130 V. However, at the cryogenic

#193788 - $15.00 USD Received 17 Jul 2013; revised 29 Aug 2013; accepted 29 Aug 2013; published 16 Sep 2013

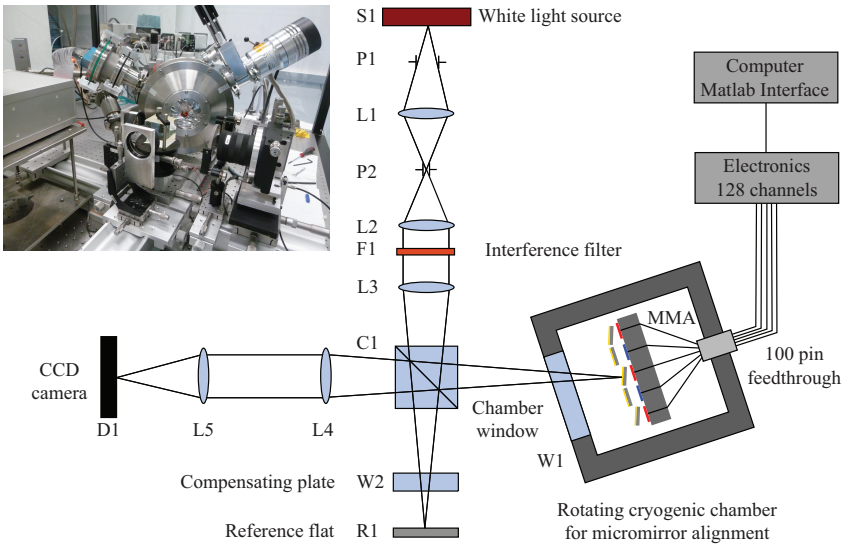

Fig. 5. Optical setup for the characterization of the micromirror surface deformation at RT and cryogenic temperatures. The MMA was placed in a cryogenic chamber, which was mounted in front of a Twyman-Green interferometer. The use of a compensating plate in the reference arm of the interferometer enabled measurements with nanometer resolution.

temperature (162 K), 130 V was not sufficient for tilting all the micromirrors, as shown in Figs. 6(b) and 6(c). Increasing the actuation voltage to 148 V enabled an additional micromirror to fully tilt, as represented in Fig. 6(d). Additionally, since the maximum output voltage of the electronics was 148 V, it was not possible to further increase the voltage to actuate all the micromirrors of the lines. This observed increase in actuation voltage could originate from modifications of the Young's Modulus and/or carrier mobility of doped polysilicon at cryogenic temperatures, and requires further study in the future. Nonetheless, the successful actuation of these micromirrors was achieved several times at cryogenic temperatures.

Upon return to RT, the lines that were not actuated at cryogenic temperatures were successfully tilted by 25° at an actuation voltage of 130 V. However, the 96 micromirrors of the 3 lines that were actuated at 162 K demonstrated a limited range of tilt angle (few degrees) for actuation voltages above 100 V. To study the origin of this issue, further optical and electrical characterization of the device was performed. The results of these studies indicated that there were no broken mirrors or polysilicon beams, no failed gold-si eutectic bondings of the frame to the pillars, and no shorted electrodes. Based on these results and on the electro-mechanical behavior of these mirrors, we assume that the limited tilt angles of the micromirrors actuated at 162 K could be due to the stiction or deformation of the suspended beams to the back of the micromirror when the device returned to RT. However, the only way to confirm this assumption would be to locally break a single mirror and have a look at its beams. Since this destructive test can potentially damage the rest of the array, it has not yet been undertaken. The proposed mechanism of how stiction or deformation of the beams hinders the actuation of the micromirrors is as follows: the deformed suspended beams cause the micromirror to touch its stopper beam before the pull-in voltage, effectively pinning the micromirror and preventing its actuation even when the voltage is increased. Further studies are planned to better understand and avoid this failure mode.

#193788 - $15.00 USD Received 17 Jul 2013; revised 29 Aug 2013; accepted 29 Aug 2013; published 16 Sep 2013

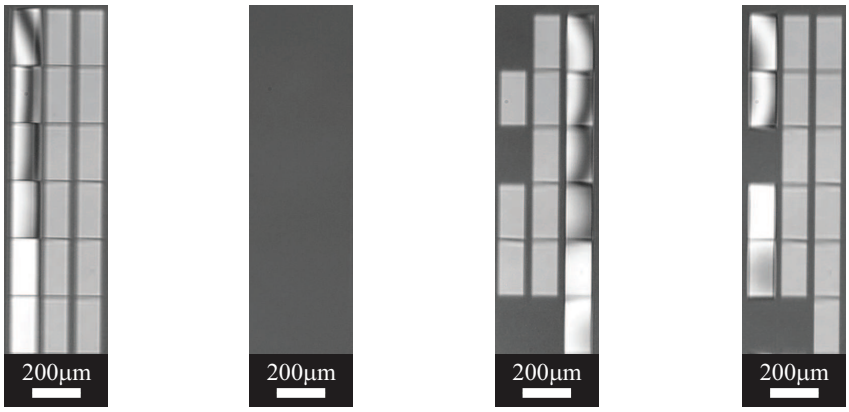

(a) (b) (c) (d)

Fig. 6. Interferometric observation of the lines of micromirrors before and during the cryogenic experiments. During this experiment, the cryogenic chamber was rotated by a value equal to the micromirror tilt angle. Therefore, the tilted micromirrors appear white (ON state), while the micromirrors at rest appear black (OFF state). Due to low coherence light, only one line of micromirror could be measured at once. Actuation of the micromirrors was successfully demonstrated at 162 K. (a) Temperature: RT, Voltage: 130 V. (b) Temperature: 162 K, Voltage: 0 V. (c) Temperature: 162 K, Voltage: 130 V. (d) Temperature: 162 K, Voltage: 148 V.

3.3.3. Deformation

The deformation of the micromirrors originates from two sources: the internal stress in a micromirror and the stress generated by the surface coating. Since silicon is transparent to infrared light, the silicon micromirrors were coated with 10 nm Ti and 50 nm Au. Due to the coefficient of thermal expansion (CTE) mismatch between silicon and the surface coating, the thickness of the micromirror (200 x 100 x 10 μm^3) was defined to ensure that its deformation at cryogenic temperatures will remain within constraints ($<$ 50 nm PTV).

The deformation of a micromirror from one of the 3 lines previously selected was measured by phase-shifting interferometry before the cryogenic test (at RT) and during the test at 162 K. Since the line of this sample did not fully tilt upon return to RT, a comparable mirror from a neighboring line was measured. Figure 7 presents the mirror deformation measurements. Before the experiment (at RT), the sample micromirror had a PTV deformation over its surface of 8 nm. At 162 K, the PTV deformation increased to 27 nm due to the CTE mismatch. After the cryogenic experiment, back at RT, a neighboring micromirror had a deformation of 10 nm. Table 1 summarizes these results.

This experiment showed that the micromirrors were slightly deformed during the cryogenic tests, and their initial optical properties were restored after cooling. After the test, optical inspection of the mirrors revealed no delamination of the gold coating, indicating the high quality of the coating. Finally, the micromirror deformation at 162 K was below the 50 nm threshold set for MOS, and if necessary, an additional coating can be deposited on the back of the micromirrors to further reduce the micromirror deformation. Therefore, our measurements indicate that the micromirrors reported here perform within the optical constraints required by MOS.

#193788 - $15.00 USD Received 17 Jul 2013; revised 29 Aug 2013; accepted 29 Aug 2013; published 16 Sep 2013

Table 1. PTV and root-mean-square (RMS) micromirror surface deformation before, during, and after the cryogenic test at 162 K. The measurements before and during the cryogenic test were made on the same micromirror. After the cryogenic test, a comparable micromirror was measured because the line previously observed did not fully tilt.

Temperature	RT (before cooling)	162 K	RT (after cooling)
Mirror state	Tilted	Tilted	Tilted
PTV deformation	8 nm	27 nm	10 nm
RMS deformation	2 nm	5 nm	1.5 nm

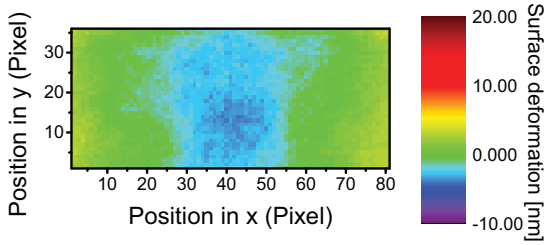

(a)

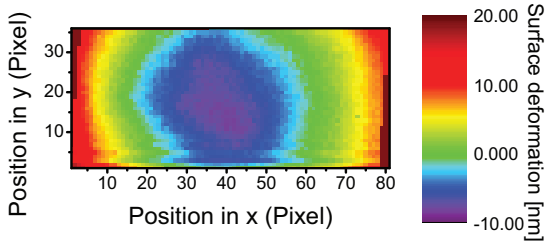

(b)

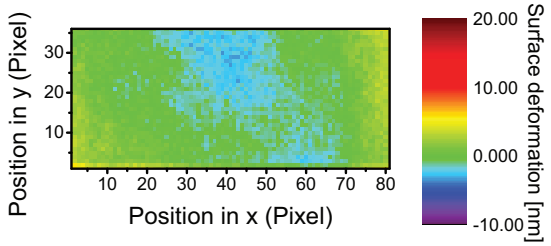

(c)

Fig. 7. Micromirror surface deformation measured by phase-shifting interferometry before, during, and after the cryogenic experiment. The silicon micromirror measuring 200 x 100 x 10 μm^3 was coated with 10 nm Ti and 50 nm Au, and was in its tilted position. (a) PTV deformation of 8 nm at RT before cooling. (b) PTV deformation of 27 nm at 162 K. (c) PTV deformation of 10 nm at RT after cooling.

#193788 - $15.00 USD Received 17 Jul 2013; revised 29 Aug 2013; accepted 29 Aug 2013; published 16 Sep 2013

4. Conclusion

In this paper, we presented the optical results of a microfabricated MMA dedicated as a reconfigurable slit mask for MOS. This device was composed of 32 x 64 micromirrors measuring 200 x 100 x 10 μm^3 and tilting by 25° at an applied potential of 130 V. The experimental results demonstrated that the MMA has optical performance above all requirements, such as a fill factor of 82% (98% in the long slit direction), a contrast ratio of 1000:1, and a PTV deformation of a coated micromirror of 27 nm at 162 K. Moreover, several lines of micromirrors were tilted by 25° at an actuation voltage of 148 V at 162 K.

In the future, to improve the reliability of the MMA, further testing at cryogenic temperatures will be performed. Also, the size of the array will be increased using the scalable fabrication process developed for this device. In addition, a space-compatible electronics for local and individual actuation of each micromirror will be developed and integrated in the array. Finally, the MMA will be tested into a MOS instrument demonstrator.

Acknowledgments

The authors would like to acknowledge the Division C staff at CSEM (Centre Suisse d'Electronique et de Microtechnique) and the CMI (Center of Microtechnology) staff at EPFL, for their support during the fabrication of the devices as well as the staff of Service Essais at LAM for the tests at cryogenic temperatures. Finally, we acknowledge R. Li and I. Y. Stein from Massachusetts Institute of Technology for helpful discussions and support.

#193788 - $15.00 USD Received 17 Jul 2013; revised 29 Aug 2013; accepted 29 Aug 2013; published 16 Sep 2013